Characterization of Imidazolate-Bridged Dinuclear and Mononuclear Hydroperoxo Complexes

Hideki Ohtsu,[1a] Shinobu Itoh,[1b] Shigenori Nagatomo,[1c] Teizo Kitagawa,[1c] Seiji Ogo,[1c] Yoshihito Watanabe,[1c] and Shunichi Fukuzumi*,[1a]

Department of Material and Life Science, Graduate School of Engineering, Osaka University, CREST, Japan Science and Technology Corporation, Suita, Osaka 565-0871, Japan, Department of Chemistry, Faculty of Science, Osaka City University, 3-3-138 Sugimoto, Sumiyoshi-ku, Osaka 558-8585, Japan, and Institute for Molecular Science, Myodaiji, Okazaki 444-8585, Japan

Received September 13, 2000

Dinucleating ligands having two metal-binding sites bridged by an imidazolate moiety, Hbdpi, HMe_2bdpi, and HMe_4bdpi (Hbdpi = 4,5-bis(di(2-pyridylmethyl)aminomethyl)imidazole, HMe_2bdpi = 4,5-bis((6-methyl-2-pyridylmethyl)(2-pyridylmethyl)aminomethyl)imidazole, HMe_4bdpi = 4,5-bis(di(6-methyl-2-pyridylmethyl)-aminomethyl)imidazole), have been designed and synthesized as model ligands for copper−zinc superoxide dismutase (Cu,Zn−SOD). The corresponding mononucleating ligands, $MeIm(Py)_2$, $MeIm(Me)_1$, and $MeIm(Me)_2$ ($MeIm(Py)_2$ = (1-methyl-4-imidazolylmethyl)bis(2-pyridylmethyl)amine, $MeIm(Me)_1$ = (1-methyl-4-imidazolyl-methyl)(6-methyl-2-pyridylmethyl)(2-pyridylmethyl)amine, $MeIm(Me)_2$ = (1-methyl-4-imidazolyl-methyl)bis(6-methyl-2-pyridylmethyl)amine), have also been synthesized for comparison. The imidazolate-bridged Cu(II)−Cu(II) homodinuclear complexes represented as $[Cu_2(bdpi)(CH_3CN)_2](ClO_4)_3\cdot CH_3CN\cdot 3H_2O$ (**1**), $[Cu_2(Me_2bdpi)-(CH_3CN)_2](ClO_4)_3$ (**2**), $[Cu_2(Me_4bdpi)(H_2O)_2](ClO_4)_3\cdot 4H_2O$ (**3**), a Cu(II)−Zn(II) heterodinuclear complex of the type of $[CuZn(bdpi)(CH_3CN)_2](ClO_4)_3\cdot 2CH_3CN$ (**4**), Cu(II) mononuclear complexes of $[Cu(MeIm(Py)_2)(CH_3-CN)](ClO_4)_2\cdot CH_3CN$ (**5**), $[Cu(MeIm(Me)_1)(CH_3CN)](ClO_4)_2$ (**6**), and $[Cu(MeIm(Me)_2)(CH_3CN)](ClO_4)_2$ (**7**) have been synthesized and the structures of complexes **5**−**7** determined by X-ray crystallography. The complexes **1**−**7** have a pentacoordinate structure at each metal ion with the imidazolate or 1-methylimidazole nitrogen, two pyridine nitrogens, the tertiary amine nitrogen, and a solvent (CH_3CN or H_2O) which can be readily replaced by a substrate. The reactions between complexes **1**−**7** and hydrogen peroxide (H_2O_2) in the presence of a base at −80 °C yield green solutions which exhibit intense bands at 360−380 nm, consistent with the generation of hydroperoxo Cu(II) species in all cases. The resonance Raman spectra of all hydroperoxo intermediates at −80 °C exhibit a strong resonance-enhanced Raman band at 834−851 cm^{-1}, which shifts to 788−803 cm^{-1} ($\Delta\nu$ = 46 cm^{-1}) when ^{18}O-labeled H_2O_2 was used, which are assigned to the O−O stretching frequency of a hydroperoxo ion. The resonance Raman spectra of hydroperoxo adducts of complexes **2** and **6** show two Raman bands at 848 (802) and 834 (788), 851 (805), and 835 (789) cm^{-1} (in the case of $H_2{}^{18}O_2$, $\Delta\nu$ = 46 cm^{-1}), respectively. The ESR spectra of all hydroperoxo complexes are quite close to those of the parent Cu(II) complexes except **6**. The spectrum of **6** exhibits a mixture signal of trigonal-bipyramid and square-pyramid which is consistent with the results of resonance Raman spectrum.

Introduction

Coordination chemistry of copper complexes is a subject of continuing importance in connection with the structures and the reactivities of the active site in copper-containing metalloproteins.[2] In particular, copper−zinc superoxide dismutase (Cu,Zn−SOD) contains an imidazolate-bridged Cu(II)−Zn(II) heterodinuclear metal center in its active site.[3−8] The copper ion is coordinated to four imidazole N atoms of histidine residues and a solvent (H_2O) in a distorted square-pyramidal geometry, while the zinc ion located at a distance of 6.2 Å from the copper ion is coordinated to a carboxylato O atom of an aspartic acid residue and three imidazole N atoms of histidine residues in a distorted tetrahedral structure.[3,4] This enzyme catalyzes a very rapid two-step dismutation of toxic superoxide to dioxygen (O_2) and hydrogen peroxide (H_2O_2) through an alternate reduction and oxidation of the active-site copper ion.[7−9] An electron transfer from superoxide to Cu(II) center occurs to produce O_2 and a Cu(I) center which may be oxidized by another

* To whom correspondence should be addressed. E-mail: fukuzumi@chem.eng.osaka-u.ac.jp.

(1) (a) Osaka University. (b) Osaka City University. (c) Institute for Molecular Science.
(2) (a) Lippard, S. J. *Science* **1993**, *261*, 699. (b) Kaim, W.; Schwederski, B. *Bioinorganic Chemistry: Inorganic Elements in the Chemistry of Life*; John Wiley & Sons: New York, 1991.
(3) (a) Fridovich, I. *J. Biol Chem.* **1989**, *264*, 7761. (b) Fridovich, I. *Annu. Rev. Biochem.* **1995**, *64*, 97.
(4) (a) Bertini, I.; Banci, L.; Piccioli, M. *Coord. Chem. Rev.* **1990**, *100*, 67. (b) Bertini, I.; Mangani, S.; Viezzoli, M. S. *Adv. Inorg. Chem.* **1997**, *45*, 127.
(5) Tainer, J. A.; Getzoff, E. D.; Beem, K. M.; Richardson, J. S.; Richardson, D. C. *J. Mol. Biol.* **1982**, *160*, 181.
(6) Tainer, J. A.; Getzoff, E. D.; Richardson, J. S.; Richardson, D. C. *Nature* **1983**, *306*, 284.
(7) Hart, P. J.; Balbirnie, M. M.; Ogihara, N. L.; Nersissian, A. M.; Weiss, M. S.; Valentine, J. S.; Eisenberg, D. A. *Biochemistry* **1999**, *38*, 2167.
(8) Fielden, E. M.; Roberts, P. B.; Bray, R. C.; Lowe, D. J.; Mautner, G. N.; Rotilio, G.; Calabrese, L. *Biochem. J.* **1974**, *139*, 49.
(9) Ellerby, L. M.; Cabelli, D. E.; Graden, J. A.; Valentine, J. S. *J. Am. Chem. Soc.* **1996**, *118*, 6556.

10.1021/ic001036v CCC: $20.00
Published on Web 05/19/2001

molecule of superoxide in the presence of proton to produce H_2O_2 via a hydroperoxo Cu(II) species.[8,9] The hydroperoxo copper(II) species is a key intermediate in biological oxidations catalyzed by copper enzymes including SOD. However, hydroperoxo copper(II) complexes have rarely been characterized.[10,11]

Several imidazolate-bridged heterodinuclear complexes have so far been reported as models of Cu,Zn−SOD using two independent mononuclear complexes and a bridging imidazolate ring.[12] However, the lack of binding site of superoxide in these dinuclear complexes has precluded the characterization of the hydroperoxo copper(II) intermediate. We have recently prepared imidazolate-bridged Cu(II)−Zn(II) heterodinuclear and Cu(II)−Cu(II) homodinuclear complexes with a newly designed dinucleating ligand, Hbdpi and HMe_4bdpi (Hbdpi = 4,5-bis(di(2-pyridylmethyl)aminomethyl)imidazole, HMe_4bdpi = 4,5-bis(di(6-methyl-2-pyridylmethyl)aminomethyl)imidazole).[13] These SOD model complexes have a pentacoordinate structure in each metal ion including a solvent molecule which can be readily replaced by a substrate.

We report herein the first characterization of SOD model hydroperoxo Cu(II) intermediates generated by the reactions of H_2O_2 with the series of imidazolate-bridged Cu(II)−Cu(II) homodinuclear, Cu(II)−Zn(II) heterodinuclear complexes containing dinucleating ligands, Hbdpi, HMe_2bdpi, and HMe_4bdpi (Hbdpi = 4,5-bis(di(2-pyridylmethyl)aminomethyl)imidazole, HMe_2bdpi = 4,5-bis((6-methyl-2-pyridylmethyl)(2-pyridylmethyl)aminomethyl)imidazole, HMe_4bdpi = 4,5-bis(di(6-methyl-2-pyridylmethyl)aminomethyl)imidazole), and the corresponding Cu(II) mononuclear complexes containing mononucleating ligands, MeIm(Py)$_2$, MeIm(Me)$_1$, and MeIm(Me)$_2$ (MeIm(Py)$_2$ = (1-methyl-4-imidazolylmethyl)bis(2-pyridylmethyl)amine, MeIm(Me)$_1$ = (1-methyl-4-imidazolylmethyl)(6-methyl-2-pyridylmethyl)(2-pyridylmethyl)amine, MeIm-(Me)$_2$ = (1-methyl-4-imidazolylmethyl)bis(6-methyl-2-pyridylmethyl)amine). The structures of Cu(II) mononuclear complexes are determined by X-ray analyses.

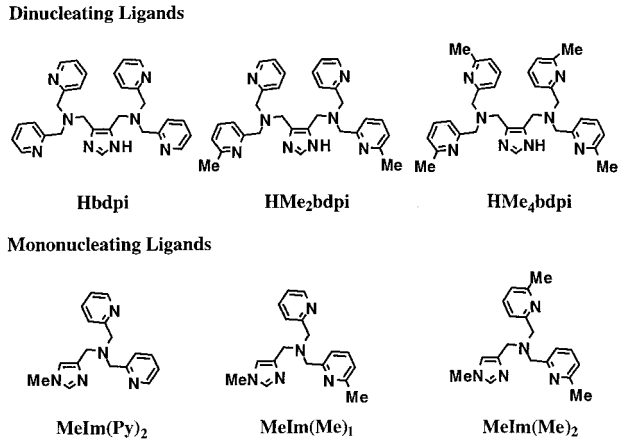

Experimental Section

Materials. All chemicals used for the ligand synthesis were commercial products of the highest available purity and were further purified by the standard methods.[14] Solvents were also purified by standard methods before use.[14]

Synthesis of Ligands. All ligands used in this study were prepared according to the following procedures, and the structures of the products were confirmed by the analytical data (vide infra).

4,5-Bis(di(2-pyridylmethyl)aminomethyl)imidazole (Hbdpi). This compound was prepared as described previously.[13]

4,5-Bis((6-methyl-2-pyridylmethyl)(2-pyridylmethyl)amino)methyl)imidazole (HMe_2bdpi). (6-Methyl-2-pyridylmethyl)(2-pyridylmethyl)amine (3.43 g, 16 mmol) and a small amount of acetic acid were added to a methanol solution (100 mL) containing imidazole-4,5-dialdehyde (1.0 g, 8 mmol). To the methanol solution was added dropwise sodium cyanoborohydride (1.0 g, 16 mmol). After the resulting solution had been stirred for 3 days at room temperature, it was acidified with concentrated hydrochloric acid and concentrated to dryness under a reduced pressure. The residue was dissolved in a saturated aqueous solution of Na_2CO_3 (50 mL) and extracted with three 50 mL portions of chloroform. The combined extracts were dried over Na_2SO_4 and after removal of the solvent gave a brown oily product, which was purified by silica gel chromatography with chloroform/methanol as eluent to give HMe_2bdpi. Yield: 2.94 g (70.4%). ^{1}H NMR ($CDCl_3$, 400 MHz): δ 2.52 (s, 6H, CH_3), 3.65 (s, 4H, NCH_2Im, Im = imidazole moiety), 3.71 (s, 4H, NCH_2Py, Py = pyridine moiety), 3.75 (s, 4H, NCH_2Py), 6.98 (d, 2H, Py, J = 7.2 Hz), 7.11 (m, 2H, Py), 7.29 (d, 2H, Py, J = 6.8 Hz), 7.50 (m, 4H, Py), 7.60 (td, 2H, Py, J = 1.6, 7.6 Hz), 7.65 (s, 1H, Im), 8.49 (d, 2H, Py, J = 4.4 Hz). ^{13}C NMR ($CDCl_3$; 100 MHz): δ 24.2 (CH_3), 48.2 (CH_2), 59.3 (CH_2), 59.4 (CH_2), 120.3 (Py), 121.4 (Py), 121.8(Py), 122.1 (Im), 123.3 (Py), 133.8 (Im), 136.3 (Py), 136.6 (Py), 148.6 (Py), 157.2 (Py), 158.4 (Py), 159.3 (Py).

4,5-Bis(di(6-methyl-2-pyridylmethyl)aminomethyl)imidazole (HMe_4bdpi), (1-Methyl-4-imidazolylmethyl)bis(2-pyridylmethyl)-amine (MeIm(Py)$_2$). These compounds were prepared as described elsewhere.[13]

(1-Methyl-4-imidazolylmethyl)(6-methyl-2-pyridylmethyl)(2-pyridylmethyl)amine (MeIm(Me)$_1$). (6-Methyl-2-pyridylmethyl)(2-pyridylmethyl)amine (1.70 g, 8 mmol) and a small amount of acetic acid were added to a methanol solution (100 mL) containing 1-methylimidazole-4-aldehyde (0.88 g, 8 mmol). To the methanol solution was added dropwise sodium cyanoborohydride (0.5 g, 8 mmol). After the resulting solution had been stirred for 3 days at room temperature, it was acidified with concentrated hydrochloric acid and concentrated to dryness under reduced pressure. The residue was dissolved in a saturated aqueous solution of Na_2CO_3 (50 mL) and extracted with three 50 mL portions of chloroform. The combined extracts were dried over Na_2SO_4 and after removal of the solvent gave a brown oily product, which was purified by silica gel chromatography with chloroform/methanol as eluent to give Hbdpi. Yield: 2.1 g (85.1%). ^{1}H NMR ($CDCl_3$, 400 MHz): δ 2.51 (s, 3H, CH_3Py), 3.60 (s, 3H, CH_3Im), 3.71 (s, 2H, NCH_2Im), 3.85 (s, 2H, NCH_2Py), 3.87 (s, 2H, NCH_2Py), 6.88 (s, 1H, Im), 6.97 (d, 1H, Py, J = 7.6 Hz), 7.10 (m, 1H, Py), 7.36 (s, 1H, Im), 7.48 (d, 1H, Py, J = 7.6 Hz), 7.53 (t, 1H, Py, J = 7.2 Hz), 7.63 (m, 1H, Py), 7.65 (m, 1H, Py), 8.50 (m, 1H, Py). ^{13}C NMR ($CDCl_3$; 100 MHz): δ 23.9 (CH_3Py), 32.8 (CH_3Im), 51.2 (CH_2), 59.2 (CH_2), 59.4 (CH_2), 118.4 (Im), 119.2 (Py), 120.8 (Py), 121.3 (Py), 122.4 (Py), 135.9 (Py), 136.2 (Py), 136.8 (Im), 138.9 (Im), 148.3 (Py), 156.9 (Py), 158.8 (Py), 159.6 (Py).

(1-Methyl-4-imidazolylmethyl)bis(6-methyl-2-pyridylmethyl)-amine (MeIm(Me)$_2$). The same procedure as that for the synthesis of MeIm(Me)$_1$ was employed to obtain MeIm(Me)$_2$ using bis(6-methyl-

(10) (a) Karlin, K. D.; Ghosh, R.; Cruse, R. W.; Farooq, A.; Gultneh, Y.; Jacobson, R. R.; Blackburn, N. J.; Strange, R. W.; Zubieta, J. *J. Am. Chem. Soc.* **1988**, *110*, 6769. (b) Tahir, R. R.; Murthy, N. N.; Karlin, K. D.; Blackburn, N. J.; Shaikh, S. N.; Zubieta, J. *Inorg. Chem.* **1992**, *31*, 3001. (c) Wada, A.; Harata, M.; Hasegawa, K.; Jitsukawa, K.; Masuda, H.; Mukai, M.; Kitagawa, T.; Einaga, H. *Angew. Chem., Int. Ed. Engl.* **1998**, *37*, 798.

(11) For a preliminary report on synthesis, see: Ohtsu, H.; Itoh, S.; Nagatomo, S.; Kitagawa, T.; Ogo, S.; Watanabe, Y.; Fukuzumi, S. *J. Chem. Soc., Chem. Commun*. **2000**, 1051.

(12) (a) Sato, M.; Nagae, S.; Uehara, M.; Nakaya, J. *J. Chem. Soc., Chem. Commun*. **1984**, 1661. (b) Lu, Q.; Luo, Q. H.; Dai, A. B.; Zhou, Z. Y.; Hu, G. Z. *J. Chem. Soc., Chem. Commun*. **1990**, 1429. (c) Zongwan, M.; Dong, C.; Wenxia, T.; Kaibei, Y.; Li, L. *Polyhedron* **1992**, *11*, 191. (d) Pierre, J.-L.; Chautemps, P.; Refaif, S.; Beguin, C.; Marzouki, A. E.; Serratrice, G.; Saint-Aman, E.; Rey, P. *J. Am. Chem. Soc*. **1995**, *117*, 1965. (e) Mao, Z.-W.; Chen, M.-Q.; Tan, X.-S.; Liu, J.; Tang, W.-X. *Inorg. Chem*. **1995**, *34*, 2889.

(13) Ohtsu, H.; Shimazaki, Y.; Odani, A.; Yamauchi, O.; Itoh, S.; Fukuzumi, S. *J. Am. Chem. Soc.* **2000**, *122*, 5733.

(14) Perrin, D. D.; Armarego, W. L. F.; Perrin, D. R. *Purification of Laboratory Chemicals*; Pergamon Press: Elmsford, U.K., 1966.

Table 1. Crystal Data for Complexes **5**−**7**

	5	**6**	**7**
formula	$CuO_8C_{21}H_{25}Cl_2N_7$	$CuO_8C_{23}H_{24}Cl_2N_6$	$CuO_8C_{22}H_{21}Cl_2N_6$
fw	637.92	646.93	631.90
color	green	blue	blue
cryst size/mm	0.30 × 0.30 × 0.40	0.30 × 0.30 × 0.20	0.30 × 0.30 × 0.10
cryst syst	monoclinic	monoclinic	monoclinic
space group	$P2_1/n$	$P2_1/c$	$P2_1/c$
a/Å	14.861(5)	13.995(5)	14.231(5)
b/Å	10.784(5)	09.192(4)	10.413(5)
c/Å	35.597(4)	20.378(3)	19.402(4)
β/deg	90.57(2)	97.47(2)	109.92(2)
V/Å^3	5704(3)	2599(1)	2703(1)
Z	8	4	4
D_c/(g cm^{-3})	1.485	1.653	1.553
radiation	Mo Kα (λ = 0.710 69 Å)	Mo Kα (λ = 0.710 69 Å)	Mo Kα (λ = 0.710 69 Å)
μ/cm^{-1}	10.08	11.07	10.62
F(000)/e	2616.00	1324.00	1288.00
scan method	$\omega-2\theta$	$\omega-2\theta$	$\omega-2\theta$
$2\theta_{max}$/deg.	50.2	55.0	55.0
scan speed/(deg. min^{-1})	16.0	16.0	8.0
scan range/deg.	0.79 + 0.30 tan θ	1.68 + 0.30 tan θ	1.15 + 0.30 tan θ
obsd reflcns	7925	6190	5961
independent reflcns	7786 (R_{int} = 0.026)	5953 (R_{int} = 0.036)	5718 (R_{int} = 0.026)
reflcns used	7786	5953	5718
no. of variables	704	578	596
R^a ($I > 2.00\sigma(I)$)	0.075	0.059	0.055
$R_w{}^a$ ($I > 2.00\sigma(I)$)	0.105	0.086	0.072

[a] $R = \sum(|F_o| - |F_c|)/\sum|F_o|$; $R_w = [\sum w(|F_o| - |F_c|)^2/\sum w|F_o|^2]^{1/2}$; $w = 1/\sigma^2(F_o)$.

2-pyridylmethyl)amine (1.82 g, 8 mmol) instead of (6-methyl-2-pyridylmethyl)(2-pyridylmethyl)amine. Yield: 2.50 g (97.3%). ^{1}H NMR ($CDCl_3$, 400 MHz): δ 2.51 (s, 6H, CH_3Py), 3.62 (s, 3H, CH_3Im), 3.69 (s, 2H, NCH_2Im), 3.83 (s, 4H, NCH_2Py), 6.87 (s, 1H, Im), 6.97 (d, 2H, Py, J = 5.2 Hz), 7.36 (s, 1H, Im), 7.48 (d, 2H, Py, J = 5.2 Hz), 7.53 (t, 2H, Py, J = 5.2 Hz). ^{13}C NMR ($CDCl_3$; 100 MHz): δ 24.1 (CH_3Py), 33.0 (CH_3Im), 51.3 (CH_2), 59.5 (CH_2), 118.5 (Im), 119.4 (Py), 120.9 (Py), 136.3 (Py), 137.0 (Im), 139.3 (Im), 157.0 (Py), 159.1 (Py).

[Cu$_2$(bdpi)(CH$_3$CN)$_2$](ClO$_4$)$_3$·CH$_3$CN·3H$_2$O (1). This complex was prepared as described previously.[13]

[Cu$_2$(Me$_2$bdpi)(CH$_3$CN)$_2$](ClO$_4$)$_3$ (2) was prepared in the same manner as that for the synthesis of **1** using the HMe$_2$bdpi ligand instead of Hbdpi. Yield: 0.666 g (65%). Anal. Calcd for $C_{35}H_{39}N_{10}Cu_2Cl_3O_{12}$: C, 41.00; H, 3.83; N, 13.66. Found: C, 41.09; H, 3.68; N, 13.74. MS data: m/z 843 [M − ClO$_4$]$^+$.

[Cu$_2$(Me$_4$bdpi)(H$_2$O)$_2$](ClO$_4$)$_3$·4H$_2$O (3), [CuZn(bdpi)(CH$_3$CN)$_2$](ClO$_4$)$_3$·2CH$_3$CN (4), and [Cu(MeIm(Py)$_2$)(CH$_3$CN)](ClO$_4$)$_2$·CH$_3$CN (5). These complexes were prepared as described previously.[13]

[Cu(MeIm(Me)$_1$)(CH$_3$CN)](ClO$_4$)$_2$ (6) was prepared in the same manner as that for the synthesis of **5** using the MeIm(Me)$_1$ ligand instead of MeIm(Py)$_2$. Yield: 0.401 g (62%). Anal. Calcd for $C_{20}H_{26}N_6Cu_1Cl_2O_9$: C, 38.20; H, 4.17; N, 13.36. Found: C, 38.31; H, 3.94; N, 13.24. MS data: m/z 469 [M − ClO$_4$]$^+$.

[Cu(MeIm(Me)$_2$)(CH$_3$CN)](ClO$_4$)$_2$ (7) was prepared in the same manner as that for the synthesis of **5** using the MeIm(Me)$_2$ ligand instead of MeIm(Py)$_2$. Yield: 0.404 g (64%). Anal. Calcd for $C_{21}H_{26}N_6Cu_1Cl_2O_8$: C, 40.36; H, 4.19; N, 13.45. Found: C, 39.86; H, 4.11; N, 13.30. MS data: m/z 483 [M − ClO$_4$]$^+$.

Safety Note. ***Caution!*** Perchlorate salts of metal complexes with organic ligands are potentially explosive and should be handled with great care.

X-ray Structure Determination. The synthesis of complexes **5**−**7** afforded well-shaped crystals suitable for X-ray diffraction study. The X-ray experiments were carried out on a Rigaku AFC-5R four-circle automated diffractometer with graphite monochromated Mo Kα radiation. The crystals were mounted on the glass capillary. The reflection intensities for **5**−**7** were monitored by three standard reflections at every 2 h and 150 measurements. The intensity decay for all the crystals was within 2%. Reflection data were corrected for both Lorentz and polarization effects. DIFABS[15] correction was applied, because the absorption coefficients (μ) for all crystals were slightly large. The structure was solved using the heavy-atom method and refined anisotropically for non-hydrogen atoms by full-matrix least-squares calculations. Each refinement was continued until all shifts were smaller than one-third of the standard deviations of the parameters involved. Atomic scattering factors were taken from the literature.[16] All hydrogen atoms located at the calculated positions, and they were assigned a fixed displacement and constrained to ideal geometry with C−H = 0.95 Å. The thermal parameters of calculated hydrogen atoms were related to those of their parent atoms by U(H) = 1.2U_{eq}(C,N). All the calculations were performed by using TEXSAN crystallographic software program package from Molecular Structure Corp. Summaries of the fundamental crystal data and experimental parameters for the structure determination of complexes **5**−**7** are given in Table 1.

Spectroscopic Studies. Electronic spectra were measured with a Hewlett-Packard HP8452A or 8453 diode array spectrophotometer with a Unisoku thermostated cell holder designed for low-temperature experiments. NMR measurements were performed with a JEOL JNM-GSX-400 (400 MHz) NMR spectrometer. Frozen solution ESR spectra were taken on a JEOL JES−RE1X X-band spectrometer, equipped with a standard low-temperature apparatus. All the spectra were recorded at 77 K in quartz tubes with 4 mm inner diameters. The g values were calibrated with a Mn(II) marker used as a reference. Resonance Raman Spectra were excited at 350.9 or 406.7 nm with Kr$^+$ laser and detected with a 1 m single polychromator (Model MC-100DG, Ritsu Oyo Kogaku) equipped with a liquid nitrogen cooled CCD detector (Model CCD3200, Astromed). The slit width and slit height were set to be 200 μm and 20 mm, respectively. The laser power used, excited at 350.9 and 406.7 nm at the sample point, was 4.0 and 6.5 mW, respectively. Raman measurements were carried out at −80 °C with a spinning cell (1000 rpm). Raman shifts were calibrated with indene, the accuracy of the peak positions of the Raman bands being ± 1 cm^{-1}. ESI mass spectra were obtained with an API 300 triple quadrupole mass spectrometer (PE-Sciex) in positive ion detection mode, equipped with an ion spray interface. The flow pass (fused silica capillary, ca. 400 mm length, 0.075 mm inner diameter) in the system was precooled by flushing with methanol cooled at −80 °C in an acetone/dry ice bath prior to measurements. A solution of hydroperoxo intermediates cooled at −80 °C was delivered to the sprayer through the fused silica capillary

(15) Walker, N.; Stuart, D. *Acta Crystallogr.* **1983**, *A39*, 158.
(16) *International Tables for X-ray Crystallography*; Kynoch Press: Birmingham, U.K., 1974; Vol. IV.

under a constant Ar pressure (0.1 MPa). The sprayer was held at a potential of 4.5 kV, and compressed N_2 was employed to assist liquid nebulization. The orifice potential was maintained at 25 V. The positive ion ESI mass spectra were measured in the range of m/z 100−1000.

Results and Discussion

Crystal Structures of Cu(II) Mononuclear Complexes. We have previously prepared the Cu(II)−Cu(II) homonuclear complexes (**1** and **3**) and the Cu(II)−Zn(II) heteronuclear complex (**4**), and the structures have been determined by X-ray crystallography. Now that we have prepared single crystals of the corresponding mononuclear Cu(II) complexes (see Experimental Section), the X-ray structures can be compared with those of the dinuclear complexes in detail.

ORTEP views of the mononuclear complexes **5**,[17] **6**, and **7** are shown in Figure 1 (parts a−c, respectively). Selected bond distances and angles of complexes **5**−**7** are summarized in Tables 2−4.

The copper ions in Cu(II) mononuclear complexes **5**−**7** have a pentacoordinate structure including a solvent molecule which can be readily replaced by a substrate as shown in Figure 1a−c, respectively). The copper center of **5** is coordinated by the 1-methylimidazole nitrogen, two pyridine nitrogens, the tertiary amine nitrogen, and a solvent nitrogen (CH_3CN). The relative amounts of the trigonal-bipyramidal component are indicated by an indexing τ representing the degree of trigonality within the structural continuum between square-pyramidal ($\tau = 0$) and trigonal-bipyramidal structures ($\tau = 1$).[18] The τ values for Cu(II) ion of **5** are obtained as $\tau = 0.96$. Thus, the coordination environment of Cu(II) ion of **5** is a trigonal-bipyramidal structure in which the 3-fold axis is comprised by N(2), N(4), and N(5) atoms with the equatorial atoms N(3) and N(6). The basal plane at the copper center comprises two pyridine nitrogens and a 1-methylimidazole nitrogen. The structure of complex **5** is similar to those of dinuclear complexes **1** and **4** with respect to the coordination geometry, in which the τ values for the Cu(II) ion of complexes **1** and **4** have been obtained as $\tau = 0.90$[19] and 0.84, respectively.[13]

The structures of complexes **6** and **7** are different from that of **5** with respect to the coordination environment of the copper center. The τ values for the Cu(II) ion of complexes **6** and **7** are obtained as $\tau = 0.15$ and 0.65, respectively. Thus, the geometry of copper ions in complexes **6** and **7** can be described as a distorted square-pyramidal structure in which the C_4 axis is comprised by N(2), N(3), N(4) and N(6) atoms. The basal plane at the copper center comprises a pyridine nitrogen, a 1-methylimidazole nitrogen, a tertiary amine nitrogen, and a solvent nitrogen (CH_3CN). It should be noted that the Cu(1)−N(5) distances in complexes **6** and **7** are significantly longer than the other Cu−N(pyridine) distances in these complexes. This is consistent with N(5) being the apexes of the pseudo-square-pyramids for Jahn−Teller distortions owing to the steric effect of the *o*-methyl group.[20] The apical Cu−N(pyridine) distance (2.320(6) Å) of **6** is the longest among the present complexes. The structure of complex **7** is quite similar to those of dinuclear complexes **3** with respect to the coordination geometry, in which the τ value for the Cu(II) ion of complex **3** is obtained as $\tau = 0.52$.[13,19]

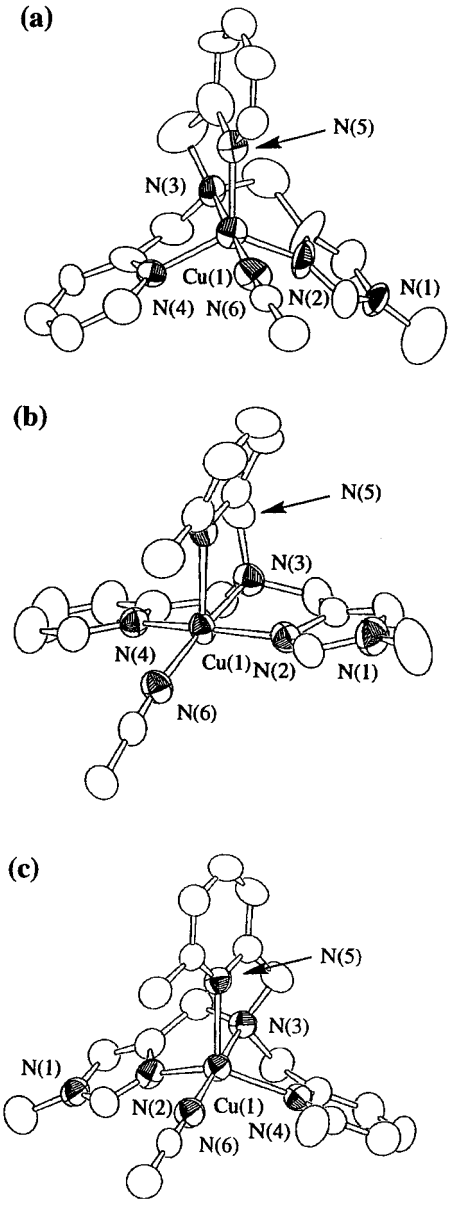

Figure 1. ORTEP views of mononuclear complexes of (a) [Cu(MeIm-(Py)$_2$)(CH_3CN)](ClO_4)$_2$·CH_3CN (**5**),[17] (b) [Cu (MeIm(Me)$_1$)(CH_3CN)]-(ClO_4)$_2$ (**6**), and (c) [Cu(MeIm(Me)$_2$)(CH_3CN)](ClO_4)$_2$ (**7**). The hydrogen atoms are omitted for clarity.

Reactions of H_2O_2 with Imidazolate-Bridged Cu(II)−Cu-(II) Homodinuclear, Cu(II)−Zn(II) Heterodinuclear, and Cu(II) Mononuclear Complexes. The Cu(II)−Cu(II) homodinuclear (**1**−**3**), Cu(II)−Zn(II) heterodinuclear (**4**), and Cu(II) mononuclear (**5**) complexes exhibit catalytic activity toward the dismutation of superoxide anions.[13] In particular, the imidazolate-bridged Cu(II)−Zn(II) heterodinuclear SOD model complex **4**, which has the binding site of superoxide ion exhibits the highest activity among the structurally established SOD models reported so far.[13] In the SOD model reactions, the hydroperoxo copper(II) complexes may be formed as the reactive intermediates.[13] The formation of the hydroperoxo copper(II) complexes is examined by the reactions of H_2O_2 with **1**−**7** (vide infra).

Absorption Spectra. The addition of a large excess of H_2O_2 to a methanol (MeOH) solution of dinuclear complexes, [Cu_2(bdpi)(CH_3CN)$_2$](ClO_4)$_3$·CH_3CN·3H_2O (**1**), [Cu_2(Me$_2$-

(17) The X-ray analysis shows that there are two independent molecules (molecules 1 and 2) of complex **5** in an asymmetric unit as shown in Table 2. Their main structural features and metric parameters are nearly identical.

(18) Addison, A. W.; Rao, T. N.; Reedijk, J.; Rijin, J.; Verschoor, G. C. *J. Chem. Soc., Dalton Trans.* **1984**, 1349.

(19) The averaged value is given for the τ values for two metal centers.

(20) Nagao, H.; Komeda, N.; Mukaida, M.; Suzuki, M.; Tanaka, K. *Inorg. Chem.* **1996**, *35*, 6809.

Table 2. Selected Bond Distances and Angles of Complex **5**[a]

molecule 1		molecule 2	
Bond Distances (Å)			
Cu(1)−N(2)	2.01(1)	Cu(2)−N(8)	2.00(1)
Cu(1)−N(3)	2.03(1)	Cu(2)−N(9)	2.03(1)
Cu(1)−N(4)	2.05(1)	Cu(2)−N(10)	2.02(1)
Cu(1)−N(5)	2.07(1)	Cu(2)−N(11)	2.06(1)
Cu(1)−N(6)	2.00(1)	Cu(2)−N(12)	1.95(1)
Bond Angles (deg)			
N(2)−Cu(1)−N(3)	81.4(7)	N(8)−Cu(2)−N(9)	83.3(7)
N(2)−Cu(1)−N(4)	119.8(6)	N(8)−Cu(2)−N(10)	120.4(6)
N(2)−Cu(1)−N(5)	117.2(6)	N(8)−Cu(2)−N(11)	117.1(7)
N(2)−Cu(1)−N(6)	96.3(8)	N(8)−Cu(2)−N(12)	97.4(8)
N(3)−Cu(1)−N(4)	82.3(6)	N(9)−Cu(2)−N(10)	82.7(7)
N(3)−Cu(1)−N(5)	83.3(6)	N(9)−Cu(2)−N(11)	81.5(7)
N(3)−Cu(1)−N(6)	177.6(7)	N(9)−Cu(2)−N(12)	179.2(8)
N(4)−Cu(1)−N(5)	117.7(6)	N(10)−Cu(2)−N(11)	117.5(6)
N(4)−Cu(1)−N(6)	98.6(7)	N(10)−Cu(2)−N(12)	96.6(8)
N(5)−Cu(1)−N(6)	98.3(7)	N(11)−Cu(2)−N(12)	98.5(8)

[a] The numbering scheme for molecule 2 follows that assigned for molecule 1.

Table 3. Selected Bond Distances and Angles of Complex **6**

Bond Distances (Å)			
Cu(1)−N(2)	1.967(5)	Cu(1)−N(5)	2.320(6)
Cu(1)−N(3)	2.074(5)	Cu(1)−N(6)	1.999(6)
Cu(1)−N(4)	1.988(5)		
Bond Angles (deg)			
N(2)−Cu(1)−N(3)	84.1(2)	N(3)−Cu(1)−N(5)	81.0(2)
N(2)−Cu(1)−N(4)	161.8(2)	N(3)−Cu(1)−N(6)	170.5(2)
N(2)−Cu(1)−N(5)	84.6(2)	N(4)−Cu(1)−N(5)	103.3(2)
N(2)−Cu(1)−N(6)	97.7(2)	N(4)−Cu(1)−N(6)	95.4(2)
N(3)−Cu(1)−N(4)	81.0(2)	N(5)−Cu(1)−N(6)	108.4(2)

Table 4. Selected Bond Distances and Angles of Complex **7**

Bond Distances (Å)			
Cu(1)−N(2)	1.982(8)	Cu(1)−N(5)	2.231(7)
Cu(1)−N(3)	2.020(7)	Cu(1)−N(6)	1.957(8)
Cu(1)−N(4)	2.080(7)		
Bond Angles (deg)			
N(2)−Cu(1)−N(3)	82.3(3)	N(3)−Cu(1)−N(5)	79.1(3)
N(2)−Cu(1)−N(4)	136.2(3)	N(3)−Cu(1)−N(6)	175.4(3)
N(2)−Cu(1)−N(5)	105.5(3)	N(4)−Cu(1)−N(5)	109.9(3)
N(2)−Cu(1)−N(6)	94.0(3)	N(4)−Cu(1)−N(6)	101.1(3)
N(3)−Cu(1)−N(4)	80.0(3)	N(5)−Cu(1)−N(6)	104.5(3)

bdpi)$(CH_3CN)_2](ClO_4)_3$ (**2**), $[Cu_2(Me_4bdpi)(H_2O)_2](ClO_4)_3 \cdot 4H_2O$ (**3**), and $[CuZn(bdpi)(CH_3CN)_2](ClO_4)_3 \cdot 2CH_3CN$ (**4**) and mononuclear complexes of $[Cu(MeIm(Py)_2)(CH_3CN)](ClO_4)_2 \cdot CH_3CN$ (**5**), $[Cu(MeIm(Me)_1)(CH_3CN)](ClO_4)_2$ (**6**), and $[Cu(MeIm(Me)_2)(CH_3CN)](ClO_4)_2$ (**7**) in the presence of a base such as triethylamine at −80 °C resulted in color change form greenish blue to green. The absorption spectra of the resulting solutions of dinuclear and mononuclear complexes are shown in Figures 2 and 3, respectively. An intense band at 360 nm of the intermediates **1a**−**4a** is observed in each dinuclear complexes **1**−**4**, as well as at 380 nm of the intermediates **5a**−**7a** in each mononuclear complexes **5**−**7**. The absorption maxima at 380 nm of **5a**−**7a** are the same as that of mononuclear hydroperoxo Cu(II) complex [Cu(II)(bppa)(OOH)](ClO_4) (bppa = bis(6-pivalamide-2-pyridylmethyl)(2-pyridylmethyl)amine), which is the only example of a structurally characterized hydroperoxo Cu(II) complex.[10c] The intense absorption band at 380 nm has been assigned to the charge-transfer transition of the hydroperoxo group to copper(II) ion (LMCT).[10c] The absorption coefficient of the band at 360 nm of the dinuclear intermediates **1a**−**4a** are slightly blue-shifted as compared to those of the mononuclear intermediates. The extinction coefficient of the absorption band at 360 nm of the intermediate **4a** derived from the Cu(II)−Zn(II) heterodinuclear complex **4** is about half as compared to those of the intermediates **1a**−**3a** derived from Cu(II)−Cu(II) homodinuclear complexes **1**−**3** (Figure 2), being comparable to those of the mononuclear intermediates (Figure 3). This is consistent with the assignment of the absorption bands as the charge-transfer transition of the hydroperoxo group to copper(II) ion (LMCT) in the intermediates, since **1a**−**3a** contain two Cu−OOH bonds, whereas **4a** has only one Cu−OOH bond. No decay of the absorption bands due to the Cu−OOH complexes was observed at −80 °C, but they disappeared when the temperature was raised to room temperature.

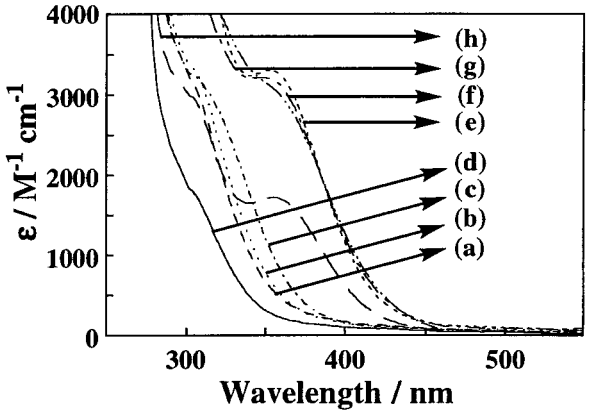

Figure 2. Absorption spectra of (a) complexes **1** (0.2 mM), (b) **2** (0.2 mM), (c) **3** (0.2 mM), and (d) **4** (0.2 mM) and those observed upon addition of a large excess H_2O_2 to a MeOH solution of (e) **1**, (f) **2**, (g) **3**, and (h) **4** in the presence of triethylamine at −80 °C.

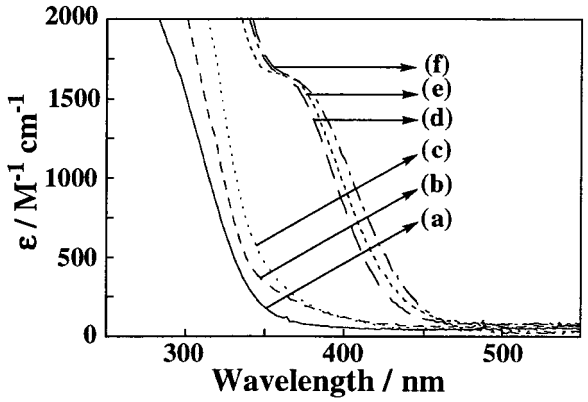

Figure 3. Absorption spectra of (a) complexes **5** (0.2 mM), (b) **6** (0.2 mM), and (c) **7** (0.2 mM) and those observed upon addition of a large excess H_2O_2 to a MeOH solution of (d) **5**, (e) **6**, and (f) **7** in the presence of triethylamine at −80 °C.

Resonance Raman Spectra. The resonance Raman spectra of dinuclear intermediates **1a**−**4a** and mononuclear intermediates **5a**−**7a** in MeOH solution at −80 °C (laser excitation wavelength 350.9 or 406.7 nm) are shown in Figures 4 a−h and 5a−f, respectively.

A strong resonance-enhanced Raman band of **1a** at 848 cm^{-1} is shifted to 802 cm^{-1} ($\Delta\nu = 46$ cm^{-1}) when ^{18}O-labeled H_2O_2 is used (Figure 4a,b). The resonance Raman spectrum of **4a** in Figure 4g,h is essentially the same as the spectrum of **1a** ($H_2{}^{16}O_2$, 848 cm^{-1}; $H_2{}^{18}O_2$, 802 cm^{-1}; $\Delta\nu = 46$ cm^{-1}). The $\Delta\nu$ value of **1a** is exactly the same as that of free H_2O_2.[21] Thus,

(21) (a) Bain, O.; Giguere, P. A. *Can. J. Chem.* **1955**, *33*, 527. (b) Taylor, R. C.; Cross, P. C. *J. Chem. Phys.* **1955**, *24*, 41. (c) Ahmad, S.; McCallum, J. D.; Shiemke, A. K.; Appelman, E. H.; Loehr, T. M.; Sanders-Loehr, J. *Inorg. Chem.* **1988**, *27*, 2230.

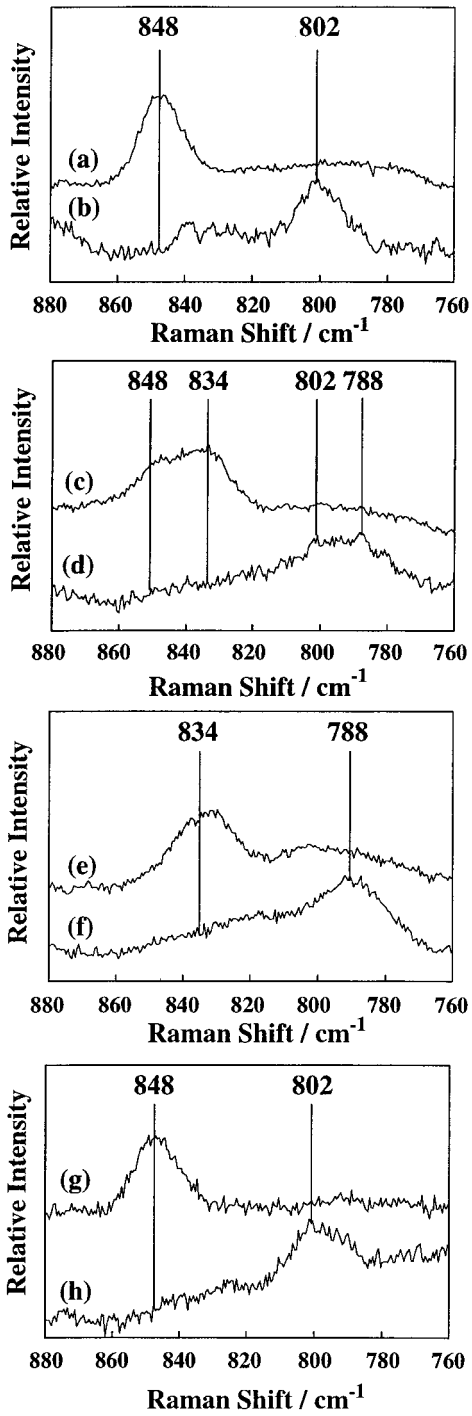

Figure 4. Resonance Raman spectra obtained with 350.9 nm excitation upon of a large excess $H_2{}^{16}O_2$ or $H_2{}^{18}O_2$ in the MeOH solution of complexes **1** [(a) $H_2{}^{16}O_2$, (b) $H_2{}^{18}O_2$], **2** [(c) $H_2{}^{16}O_2$, (d) $H_2{}^{18}O_2$], **3** [(e) $H_2{}^{16}O_2$, (f) $H_2{}^{18}O_2$], and **4** [(g) $H_2{}^{16}O_2$, (h) $H_2{}^{18}O_2$] in the presence of triethylamine at −80 °C.

the Raman band of the Cu(II)−OOH complex at 848 cm^{-1} is assigned to the O−O stretching frequency of a hydroperoxo ion, although the ν value (848 cm^{-1}) of **1a** is slightly lower than the value (856 cm^{-1}) reported for mononuclear hydroperoxo Cu(II) complex $[Cu^{II}(bppa)(OOH)](ClO_4)$.[10c]

Formation of hydroperoxo Cu(II) intermediates has been further confirmed by the ESI mass spectra of **1a** and **4a** in MeOH at −80 °C, which exhibited signals at *m*/*z* 681 and 651, respectively (see Supporting Information). The observed mass and isotope patterns correspond to the ions $[Cu_2(bdpi)(OOH)_2]^+$ and $[CuZn(bdpi)(OOH)]^+$, respectively. The use of $H_2{}^{18}O_2$ instead of $H_2{}^{16}O_2$ results in the expected change of mass numbers of **1a** and **4a** to *m*/*z* 685 and 655, respectively.

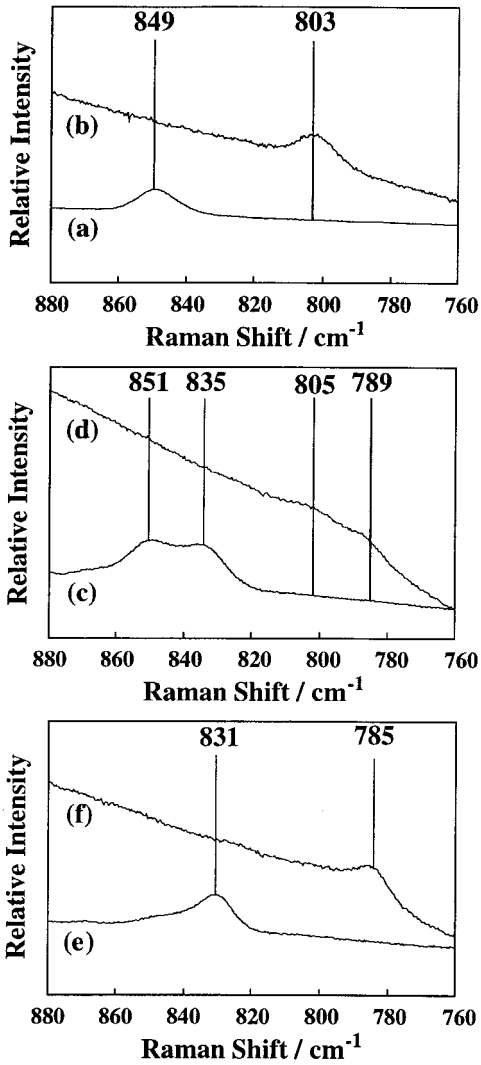

Figure 5. Resonance Raman spectra obtained with 406.7 nm excitation upon of a large excess $H_2{}^{16}O_2$ or $H_2{}^{18}O_2$ in the MeOH solution of complexes **5** [(a) $H_2{}^{16}O_2$, (b) $H_2{}^{18}O_2$], **6** [(c) $H_2{}^{16}O_2$, (d) $H_2{}^{18}O_2$], and **3** [(e) $H_2{}^{16}O_2$, (f) $H_2{}^{18}O_2$] in the presence of triethylamine at −80 °C.

The Raman band of **3a** in Figure 4e,f ($H_2{}^{16}O_2$, 834 cm^{-1}; $H_2{}^{18}O_2$, 788 cm^{-1}; $\Delta\nu = 46$ cm^{-1}) is 14 cm^{-1} lower than the values of **1a** ($H_2{}^{16}O_2$, 848 cm^{-1}; $H_2{}^{18}O_2$, 802 cm^{-1}; $\Delta\nu = 46$ cm^{-1}). This can be explained by taking into account the difference in the redox potentials between **1** and **3**. The cyclic voltammograms of complexes **1** and **3** in CH_3CN give two reversible redox waves (complex **1**, $E_{1/2a} = -0.03$ V and $E_{1/2b} = -0.31$ V; complex **3**, $E_{1/2a} = +0.12$ V and $E_{1/2b} = -0.29$ V vs Ag/AgCl).[13] Such a positive shift in the $E_{1/2a}$ value of complex **3** may be ascribed to the steric effect of 6-methyl group in the Me_4bdpi ligand in **3** which leads to the weaker coordination to the Cu(II) ion as compared to the nonsubstituted bdpi ligand in **1**,[20] indicating the lower electron density on the copper ion of **3** as compared to that of **1**. This may be the reason the O−O stretching frequency in **3a** is lower than that of **1a**. This is also consistent with the lower Raman band of **7a** in Figure 5e,f ($H_2{}^{16}O_2$, 831 cm^{-1}; $H_2{}^{18}O_2$, 785 cm^{-1}; $\Delta\nu = 46$ cm^{-1}) than that of **5a** in Figure 5a,b ($H_2{}^{16}O_2$, 849 cm^{-1}; $H_2{}^{18}O_2$, 803 cm^{-1}; $\Delta\nu = 46$ cm^{-1}).

The resonance Raman spectrum of the dinuclear intermediate **2a** derived from the reaction of **2** with $H_2{}^{16}O_2$ ($H_2{}^{18}O_2$) in Figure

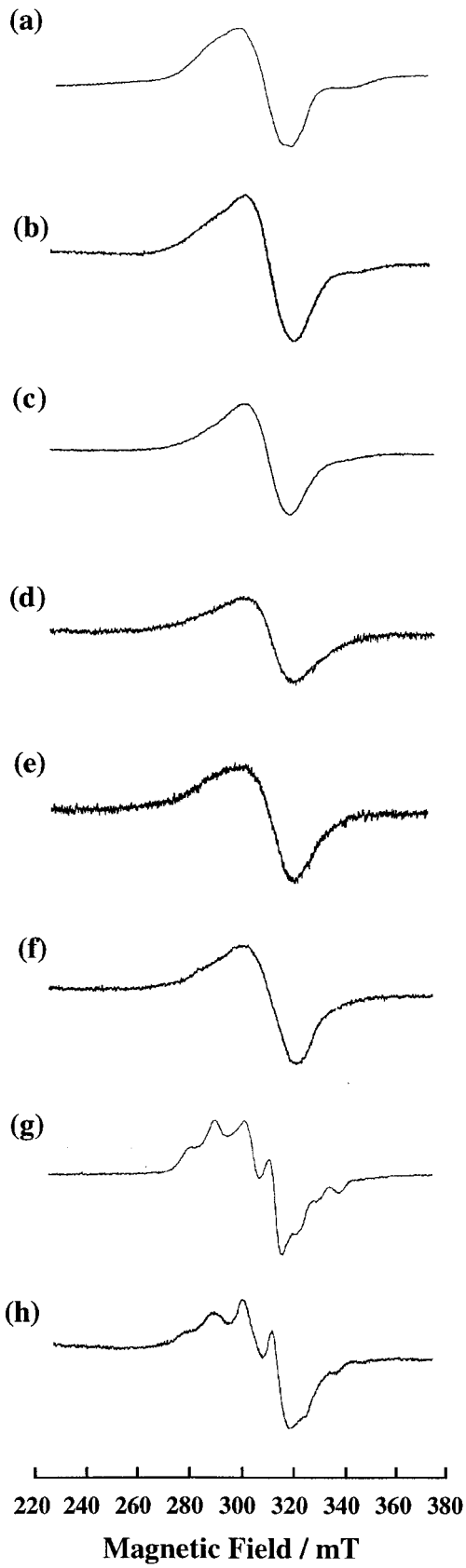

Figure 6. ESR spectra of complexes (a) **1a**, (b) **1**, (c) **2a**, (d) **2**, (e) **3a**, (f) **3**, (g) **4a,** and (h) **4** in MeOH at 77 K.

4c (Figure 4d) exhibits two Raman bands at 848 (802) and 834 (788) cm^{-1} (the values for $H_2{}^{18}O_2$ are in parentheses). Two such Raman bands are also observed for the mononuclear intermediate **6a** derived from the reaction of **6** with $H_2{}^{16}O_2$ ($H_2{}^{18}O_2$) in

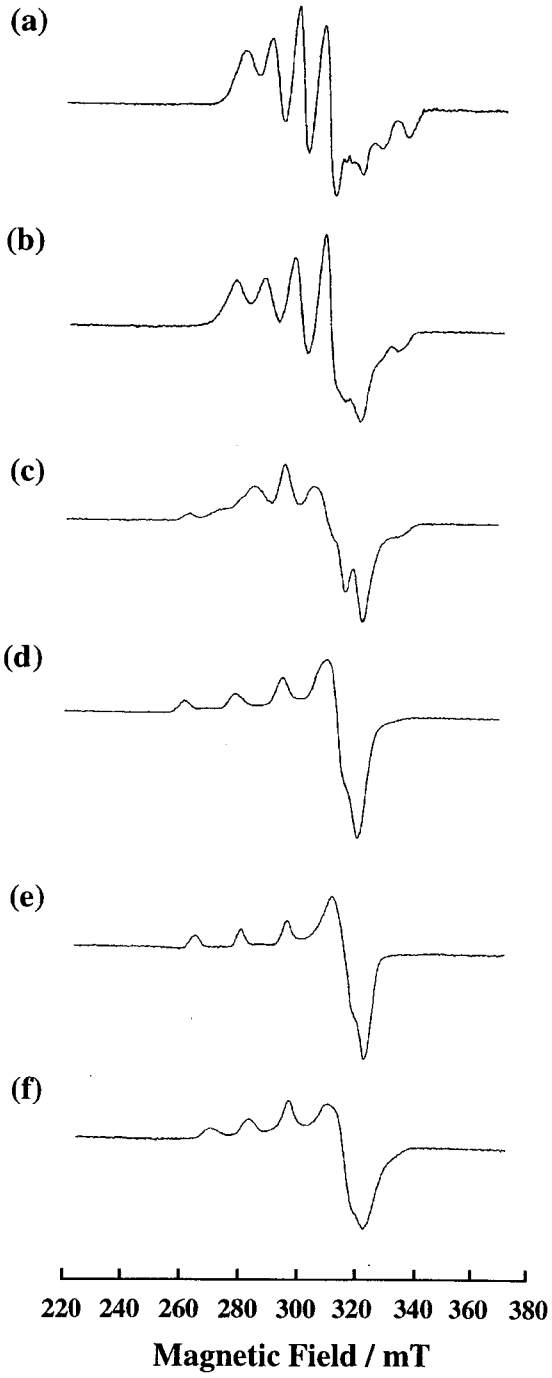

Figure 7. ESR spectra of complexes (a) **5a**, (b) **5**, (c) **6a**, (d) **6**, (e) **7a,** and (f) **7** in MeOH at 77 K.

Figure 5c (Figure 5d) at 851 (805) and 835 (789) cm^{-1} (the values for $H_2{}^{18}O_2$ are in parentheses). In each case, $\Delta\nu$ value is the same as observed for **1a** and **3a**. The origin of the two Raman bands will be discussed in the next section.

ESR Spectra. The ESR spectra of dinuclear intermediates **1a**−**4a** (0.5 mM) in MeOH at 77 K are shown in Figure 6a,c,e,g together with those of **1**−**4** in Figure 6b,d,f,h, respectively. The ESR spectra of both the dinuclear intermediates (**1a**−**3a**) and the parent complexes (**1**−**3**) exhibit a fairly broad signal centered at $g \cong 2.13$ without hyperfine structure, which is attributed to the antiferromagnetic Cu(II)−Cu(II) spin−spin interaction.[22,23]

(22) Yokoi, H.; Chikira, M. *J. Chem. Soc., Chem. Commun.* **1982**, 1125.
(23) A "$\Delta M_s = 2$" transition in the region of $g \cong 4$ was not observed because of the low intensity with the large line width.

This is consistent with the results of magnetic susceptibility.[13] The identical spectral features between the dinuclear intermediates (**1a**−**3a**) and the parent complexes (**1**−**3**) indicate that the structures of the intermediates **1a**−**3a** maintain the imidazolate-bridged structures as do the parent complexes.

On the other hand, the ESR spectrum of **4a** (Figure 6g) exhibits a typical signal of a trigonal-bipyramidal copper complex ($g_{\|} = 2.09$, $g_{\perp} = 2.22$, $|A_{\|}| = 8.9$ mT, and $|A_{\perp}| = 11.3$ mT). These ESR parameters are quite close to those of **4** in Figure 6h ($g_{\|} = 2.10$, $g_{\perp} = 2.25$, $|A_{\|}| = 10.4$ mT, and $|A_{\perp}| = 11.5$ mT). The trigonal-bipyramidal coordination environment of copper ion in **4** has been confirmed by the X-ray structure of **4**.[13] Thus, the copper coordination site of **4** occupied by a solvent molecule may be substituted with the hydroperoxide in the reaction with H_2O_2 in the presence of triethylamine base without changing the copper coordination geometry.

The ESR spectra of mononuclear intermediates **5a** and **7a** (0.5 mM) in MeOH at 77 K are shown in Figure 7a,e, from which the ESR parameters (**5a**, $g_{\|} = 2.09$, $g_{\perp} = 2.21$, $|A_{\|}| = 8.0$ mT, and $|A_{\perp}| = 9.4$ mT; **7a**, $g_{\|} = 2.26$, $g_{\perp} = 2.06$, $|A_{\|}| = 15.5$ mT) are obtained. These ESR parameters indicate that Cu(II) ion in intermediate **5a** has a trigonal-bipyramidal environment and that in **7a** has a square-pyramidal environment in agreement with the X-ray structure in Figure 1a,c (vide supra). In contrast to this, the ESR spectrum of **6a** in Figure 7c exhibits a mixed signal of trigonal-bipyramid and square-pyramid. This is consistent with two Raman bands of **6a** at 851 (805) and 835 (789) cm^{-1} (the values for $H_2{}^{18}O_2$ are in parentheses), which may be derived from the different Cu(II) coordination environment (one is trigonal-bipyramid and the other is square-pyramid). Since two Raman bands are also observed for the dinuclear complex **2a** (848 (802) and 834 (788) cm^{-1}), the two Cu(II) coordination environment in intermediate **2a** may be different from each other: one has a trigonal-bipyramidal structure and the other has a square-pyramidal structure. This can be explained by taking into account the difference in the energy level of d_{x2-y2} orbital. Complex **6** has an unpaired electron mainly in the d_{x2-y2} orbital of Cu(II) ion with a square-pyramidal structure derived from X-ray crystallography. The energy level of d_{x2-y2} orbital in **6a** may be lower than that in **6**, because the hydroperoxo ion is the weaker ligand than acetonitrile in the spectrochemical series.[24] This may be the reason the energy barriers for configrational changes between square-pyramidal and trigonal-bipyramidal is lower than other complexes.

Concluding Remarks

The present study has demonstrated for the first time that hydroperoxo Cu(II) complexes **1a**−**7a** are generally formed in the reactions of H_2O_2 with imidazolate-bridged Cu(II)−Cu(II) and Cu(II)−Zn(II) SOD model complexes **1**−**4** and corresponding mononuclear complexes **5**−**7** all of which have a binding site in the presence of triethylamine base. The hydroperoxo Cu(II) complexes characterized in this study can be regarded as SOD intermediate models.

Acknowledgment. We are grateful to Professor Osamu Yamauchi, Nagoya University (present address: Kansai University), for valuable discussions. This work was partially supported by Grants-in-Aid for Scientific Research Priority Area (Nos. 11228205, 11136229, 11116219, and 11118244) from the Ministry of Education, Science, Culture and Sports of Japan.

Supporting Information Available: Experimental and calculated peak envelopes in the positive ESI mass spectrum of $[Cu_2(bdpi)(OOH)_2]^+$ in MeOH at −80 °C (Figure S1). This material is available free of charge via the Internet at http://pubs.acs.org.

IC001036V

(24) (a) Fajans, C. J. *Naturwissenschaften* **1923**, *11*, 165. (b) Shimura, Y.; Tsuchida, R. *Bull. Chem. Soc. Jpn.* **1956**, *29*, 311.